Supporting Information (SI)

Abigail Plummer, Roberto Benzi, David R. Nelson, Federico Toschi

Contents

A. Agent-based Simulations with Advection and Diffusion

For a well-mixed system, our stochastic agent-based model for two species, A and B, uses reaction rates:

$$\text{birth of } A: \quad A \to A + A \quad \text{at rate } \mu, \tag{S1}$$
$$\text{death of } A: \quad A \to \emptyset \quad \text{at rate } \gamma(N_A - 1) + \lambda_{AB} N_B, \tag{S2}$$
$$\text{birth of } B: \quad B \to B + B \quad \text{at rate } \mu, \tag{S3}$$
$$\text{death of } B: \quad B \to \emptyset \quad \text{at rate } \gamma(N_B - 1) + \lambda_{BA} N_A, \tag{S4}$$

where N_A and N_B are the number of organisms of species A and B respectively.

We assume that birth and intraspecies death processes occur at the same rates, μ and γ, for both species, making the well-mixed carrying capacity of each species in isolation identical. Interspecies death rates can vary, however, allowing the model to capture selective advantage, mutualism, and competitive exclusion [1]. We are interested in the case of competition in the presence of selective advantage, and take, for simplicity, γ, the intraspecies death rate, to be equal to the average of λ_{AB} and λ_{BA}. The deviation from this average value, normalized by γ, is a measure of the selective advantage, s.

$$s = 1 - \frac{\lambda_{AB}}{\gamma} = \frac{\lambda_{BA}}{\gamma} - 1. \tag{S5}$$

Another common choice for selective advantage is to let $\mu \to \mu(1+s)$ for one of the species, modeling a faster growth rate. This choice represents selective advantage in dilute conditions, while Equation S5 gives selective advantage under crowded conditions [2]. Our definition simplifies our analysis because it leads to a stationary average total population size throughout the fixation process.

We extend our model to one dimension by dividing our spatial domain into intervals, and only allow organisms within the same interval to contribute to the death rates as defined above. Advection and diffusion are incorporated by allowing organism i at position x_i to move at each time step according to

$$\Delta x_i = u(x_i, t)\Delta t + \sqrt{2D\Delta t}\Gamma(t), \tag{S6}$$

where D is the diffusion constant, $u(x,t)$ is the velocity field, and $\Gamma(t)$ is a normally distributed random variable with zero mean and unit variance.

B. Macroscopic Equations

Given the microscopic reaction rates in the previous section, we can carry out a coarse-graining procedure using a Kramers-Moyal expansion for a well-mixed system [3–5]. The Fokker-Planck equation, in terms of Kramers-Moyal expansion coefficients $C_i^{(1)}(\mathbf{y})$ and $C_{ij}^{(2)}(\mathbf{y})$, is

$$\partial_t P(\mathbf{y}, t) = -\sum_i \partial_i [C_i^{(1)}(\mathbf{y}) P(\mathbf{y}, t)] + \frac{1}{2} \sum_{i,j} \partial_i \partial_j [C_{ij}^{(2)}(\mathbf{y}) P(\mathbf{y}, t)], \tag{S7}$$

with the sum over species, and $P(\mathbf{y},t)$ is the probability of being in the state $\mathbf{y}=(a,b,...)$, a vector formed from the number of organisms of each species, at time t.

For our set of reactions, we have two variables, a, the number of organisms of species A, and b, the number of organisms of species B. The Kramers-Moyal expansion coefficients for our system, using the microscopic parameters given in Section A, are

$$C_a^{(1)} = \mu a - \gamma a(a-1) - \lambda_{AB} ab \approx \mu a - \gamma a^2 - \gamma(1-s)ab, \tag{S8}$$

$$C_b^{(1)} = \mu b - \gamma b(b-1) - \lambda_{BA} ab \approx \mu b - \gamma b^2 - \gamma(1+s)ab, \tag{S9}$$

$$C_{aa}^{(2)} = \mu a + \gamma a(a-1) + \lambda_{AB} ab \approx \mu a + \gamma a^2 + \gamma(1-s)ab, \tag{S10}$$

$$C_{bb}^{(2)} = \mu b + \gamma b(b-1) + \lambda_{BA} ab \approx \mu b + \gamma b^2 + \gamma(1+s)ab, \tag{S11}$$

$$C_{ab}^{(2)} = C_{ba}^{(2)} = 0, \tag{S12}$$

where we have assumed $a, b >> 1$.

A set of stochastic differential equations associated with Equation S7 is

$$\frac{da}{dt} = C_a^{(1)} + \sqrt{C_{aa}^{(2)}}\Gamma_a(t), \tag{S13}$$

$$\frac{db}{dt} = C_b^{(1)} + \sqrt{C_{bb}^{(2)}}\Gamma_b(t), \tag{S14}$$

where the $\{\Gamma_i(t)\}$ are delta correlated Gaussian random variables such that $\langle \Gamma_i(t)\Gamma_i(t')\rangle = \delta(t-t')$ and $\langle \Gamma_i(t)\Gamma_j(t)\rangle = \delta_{ij}$. Note that the noise is multiplicative.

We now restrict our attention to the deterministic parts of Equations S13 and S14 (i.e. we neglect the noise terms), as this is all we need for the Fisher wave analysis. We follow the procedure described in detail in Pigolotti et al. [3] to add advection and diffusion terms. The equations for $a(x,t)$ and $b(x,t)$, subject to a compressible flow field $u(x,t)$ in one dimension, become

$$\frac{\partial a}{\partial t} + \partial_x(ua) = D\partial_x^2 a + \mu a - \gamma a(a+b) + s\gamma ab, \tag{S15}$$

$$\frac{\partial b}{\partial t} + \partial_x(ub) = D\partial_x^2 b + \mu b - \gamma b(a+b) - s\gamma ab. \tag{S16}$$

Upon changing variables to $f(x,t) = \frac{a}{a+b}$, the fraction of A organisms, and $c(x,t) = \frac{(a+b)\gamma}{\mu}$, the total population as a fraction of the well-mixed carrying capacity, we recover Equations 1 and 2 of the main text,

$$\frac{\partial c}{\partial t} + \partial_x(uc) = D\partial_x^2 c + \mu c(1-c), \tag{S17}$$

$$\frac{\partial f}{\partial t} + u\partial_x f = D\partial_x^2 f + \frac{2D}{c}\partial_x f \partial_x c + sc\mu f(1-f). \tag{S18}$$

Note that these equations only hold in the continuum limit. For small $a+b$, we expect these equations to break down.

C. Kimura's Formula, Extended to Higher Dimensions

To derive Equation 3 in the main text, the fixation probability, we need to work with the Kolmogorov backward equation for our system in the long time limit with the final condition that no B organisms remain. We start by deriving results for well-mixed organisms. At second order, the Kolmogorov backward equation for the well-mixed case is

$$\partial_{t'} P(\mathbf{y}',t') = \sum_i C_i^{(1)}(\mathbf{y}')\partial_i P(\mathbf{y}',t') + \frac{1}{2}\sum_{i,j} C_{ij}^{(2)}(\mathbf{y}')\partial_i\partial_j P(\mathbf{y}',t'), \tag{S19}$$

where $\mathbf{y}$, as before, is a vector of the number of organisms in the system, and $\mathbf{y}'$ is the initial state of the system at time t'.

We again change variables to $f = \frac{a}{a+b}$ and $c = \frac{(a+b)\gamma}{\mu}$. Since we are no longer neglecting noise, we first convert Equation S19 to a stochastic differential equation and then apply Ito's formula ([5], page 93). Because we expect $N = \mu/\gamma$, the well-mixed carrying capacity, to be large and s to be small, we can neglect terms that are multiplied by γs. This gives us the equations:

$$\frac{df}{dt} = sc\mu f(1-f) + \sqrt{f(1-f)\gamma\Big(\frac{c+1}{c}\Big)}\Gamma_f(t), \tag{S20}$$

$$\frac{dc}{dt} = \mu c(1-c) + \sqrt{\gamma c(c+1)}\Gamma_c(t). \tag{S21}$$

Note that Equations S20 and S21 differ in two important ways. First, if $s << 1$, Equation S20 relaxes much more slowly than Equation S21. Second, $f = 1$ is an absorbing state, whereas c can fluctuate freely around $c = 1$. We will now decouple these two equations. In the absence of noise, c is stationary at either $c = 0$ or $c = 1$, unstable and stable states respectively. To see if it is reasonable to approximate c with $c(x,t) = 1$, we linearize Equation S21 by setting $c = 1 + \varepsilon(t)$.

$$\frac{d\varepsilon}{dt} = -\mu\varepsilon + \sqrt{\frac{2\mu}{N}}\Gamma_c(t). \tag{S22}$$

This Langevin equation describes an Ornstein-Uhlenbeck process, whose stationary solution is a Gaussian with mean 0 and variance $1/N$ [5]. Because of this $1/N$ scaling, it is reasonable to neglect fluctuations in c, corresponding to a large carrying capacity, and set $\varepsilon = 0$, or $c = 1$.

Having eliminated Equation S21, Equation S20 becomes

$$\frac{df}{dt} = s\mu f(1-f) + \sqrt{\frac{2\mu}{N}f(1-f)}\Gamma_f(t), \tag{S23}$$

which corresponds to the Kolmogorov backward equation

$$\partial_{t'}P(f',t') = s\mu f'(1-f')\partial_{f'}P(f',t') + \mu\frac{f'(1-f')}{N}\partial^2_{f'}P(f',t'), \tag{S24}$$

where f' is the initial fraction of A organisms at time t'.

We can now solve this equation directly for the fixation probability, using the long time limit, with $P(f') = \lim_{t\to\infty} P(1,t|f',0)$, and the boundary conditions $P(1) = 1$ and $P(0) = 0$.

Equation S24 then leads to Kimura's formula for the fixation probability.

$$P_{fix}(s,N,f) = \frac{1-\exp(-sNf)}{1-\exp(-sN)}. \tag{S25}$$

Thus, we find that our microscopic rules result in Kimura's formula for the well-mixed case, in agreement with our numerical results.

To address the question of how Equation S25 changes when spatial structure is added, we first turn to the simpler Moran model. In the Moran model, there are a fixed number of organisms, N, and at every time step, one organism is selected to reproduce, and another is selected to die, incrementing the fraction of A organisms, f, in steps of size $1/N$. To add selective advantage, one type of organism is made more likely to be chosen for reproduction. Upon choosing A for reproduction a fraction $\frac{f(1+s)}{1+sf}$ of the time, and allowing A to die a fraction f of the time, we have

$$C^{(1)}_f = \frac{1}{N}\frac{f(1+s)}{1+sf}(1-f) - \frac{1}{N}\frac{1-f}{1+sf}(f) = \frac{sf(1-f)}{N(1+sf)} \approx \frac{sf(1-f)}{N}, \tag{S26}$$

$$C^{(2)}_{ff} = \frac{1}{N^2}\frac{f(1-f)(2+s)}{1+sf} \approx \frac{2f(1-f)}{N^2}. \tag{S27}$$

These Kramers-Moyal expansion coefficients are the same as those for our microscopic model (Sections A and B) up to a constant, and give the same fixation probability. Therefore, instead of working with our microscopic model in higher dimensions, we can work with a ring (or lattice) of well-mixed colonies in the Moran model connected by migration. Because our model and the Moran model have the same coarse-grained evolution equations at the level

of approximation we are interested in, we should be able to apply results derived for the spatially structured Moran model to our system (in the limit of large colony size).

Following Maruyama [6]'s treatment of the Moran model, we consider the moment at which the birth/death occurs in a colony l with N_l organisms, a fraction f_l of them of type A ($\sum_l f_l N_l = fN$). We will assume that the total population size is constant, as before, but we do not need to assume that the number of organisms in each cell, or even the number of cells, remains the same in between steps.

The probability that one A organism replaces one B organism in colony l is

$$r_l^+ = \frac{f_l(1+s)}{1+sf_l}(1-f_l). \tag{S28}$$

The probability that a B organism replaces an A organism is

$$r_l^- = \frac{1-f_l}{1+sf_l}f_l. \tag{S29}$$

The probability that f_l does not change is

$$r_l^0 = 1 - r_l^+ - r_l^-. \tag{S30}$$

Upon considering only events that change the number of A by 1, we can write the probability that A increased as the sum over colonies of the product of the probability that an event occurs in a colony with fraction f_l times the probability that that event was a birth,

$$p = \frac{\sum_l \frac{N_l}{N} r_l^+}{\sum_l \frac{N_l}{N} r_l^+ + \sum_l \frac{N_l}{N} r_l^-}. \tag{S31}$$

Similarly, the probability that A decreased is given by

$$q = \frac{\sum_l \frac{N_l}{N} r_l^-}{\sum_l \frac{N_l}{N} r_l^+ + \sum_l \frac{N_l}{N} r_l^-}. \tag{S32}$$

All terms have the same l dependence, which cancels. We are left with

$$p = \frac{1+s}{2+s}, \tag{S33}$$

$$q = \frac{1}{2+s}. \tag{S34}$$

We have reduced this problem to that of an unfair coin toss, where the global fraction is increased by $1/N$ with probability p and decreased by $1/N$ with probability q. The fixation probability is then the classic solution to the gambler's ruin problem, the exit probability of a biased random walker. Surprisingly, p and q are independent of the details of $\{N_l\}$, meaning that the fixation probability is independent of spatial structure as long as this argument holds. However, this argument does *not* imply any spatial structure independence of the time to fixation. Because we are only considering events that change the global fraction of A organisms, the average time between steps of the random walk varies with f.

To complete Maruyama's argument, we solve for the exit probability of a biased random walker

$$P(a) = \frac{1-(q/p)^a}{1-(q/p)^N} = \frac{1-\frac{1}{(1+s)^a}}{1-\frac{1}{(1+s)^N}} \approx \frac{1-\exp(-sa)}{1-\exp(-sN)}, \tag{S35}$$

where $a = f'N$ is the initial number of organisms of species A. This agrees with Equation S25:

$$P_{fix}(s,N,f) = \frac{1-\exp(-sNf)}{1-\exp(-sN)}. \tag{S36}$$

The derivation of the spatial structure independence of Kimura's formula relies on the assumptions that our population can be modeled as a set of well-mixed colonies and that all organisms in the population are equally likely to reproduce/die and cause the global fraction to increase/decrease. These assumptions hold on average for our model when only diffusion is added. Our birth rate is defined to always be equal for all organisms, and the death rate is concentration dependent. Since the diffusive term ensures that the concentration stays more or less uniform, this will give an approximately uniform death rate. Therefore, we expect fixation probabilities in our model to follow Kimura's formula in any dimension when only diffusive motion is included.

These assumptions can fail when a flow field is added. In particular, any flow field that, even temporarily, concentrates organisms will violate the necessary assumptions, as crowded organisms are more likely to die. For a related study of fixation probabilities in a variety of interesting flow fields, see [7].

D. Random Walk Analysis of Fixation in a Sine Wave Flow

Suppose we have a sine wave flow field with amplitude A_0. Consider the initial condition of Figure 1 in the main text, where a small number of purple organisms start in a narrow window surrounded by green organisms, both species distributed so that the total concentration is the steady state no-flow carrying capacity. Because the concentration is approximately time-independent and spatially uniform in the presence of weakly compressible flows, we can think of fixation events as the convergence of two genetic boundaries, regarded as random walkers on a ring with a spatially varying bias. If the convergence of the P|G and G|P boundaries is such that the purple sector is pinched shut, this is a fixation event for green, and vice versa (see Figure S1.A). Simulations of random walkers confirm that this simple model accurately describes our agent-based simulations.

With our sine wave flow field, there is a single source, So, at $x = \pi/2$ and a single sink, Si, at $x = 3\pi/2$. Consider the half domain symmetrically bracketing the source in the periodic domain $[0,\, 2\pi]$, as in Figure S1.B. If two random walking genetic domain walls G|P and P|G exit on opposite sides of this region, it is unlikely that they are able to return. Hence, the probability of exiting on opposite sides of the half domain before converging gives an approximate fixation probability for the purple species. We further approximate the sine wave as a linear velocity field in this half domain.

This simplified problem can be solved analytically. The two random walkers in the interval $x_s \pm \pi/2$, where x_s is the location of the source, can be mapped to the x and y coordinates of a single random walker in two dimensions, as in Figure S1.B. Without loss of generality, we set $x_s = 0$ and $y \geq x$, as the walkers are assumed to converge if they cross paths. The exit probabilities for the two-dimensional walker give the approximate fixation probabilities of our system. If the walk reaches the line $x = y$ first, convergence has occurred and green fixes. If the walk reaches the top left corner, where $x = -\pi/2, y = \pi/2$, divergence has occurred and purple fixes.

The equations for the exit probabilities, $p(x, y)$, are given by a Kolmogorov backward equation that can be derived with a first step analysis. If the random walker begins at the line $x = y$, its chance of first reaching the corner is 0. Therefore, $p(x, x) = 0$ gives one boundary condition. Similarly, $p(-\pi/2, \pi/2) = 1$. The other parts of the boundary represent the case in which one of the original random walkers has exited the half domain, but the other one remains inside. In this case, we must wait and see where the second walker decides to exit. Therefore, the boundary condition for $p(x, \pi/2)$ and $p(-\pi/2, y)$ is the solution of a one-dimensional diffusion-with-drift problem, with $p(x)$ fixed at 0 and 1 on the appropriate ends. The Kolmogorov backward equation inside the triangle reads

$$D\partial_x^2 p(x,y) + D\partial_y^2 p(x,y) + A_0 x \partial_x p(x,y) + A_0 y \partial_y p(x,y) = 0, \tag{S37}$$

with boundary conditions, (S38)

$$p(-\pi/2, y) = \frac{1}{2} + \frac{\mathrm{Erf}\Big[y\sqrt{\frac{A_0}{2D}}\Big]}{2\mathrm{Erf}\Big[\frac{\pi}{2}\sqrt{\frac{A_0}{2D}}\Big]}, \tag{S39}$$

$$p(x, \pi/2) = \frac{1}{2} - \frac{\mathrm{Erf}\Big[x\sqrt{\frac{A_0}{2D}}\Big]}{2\mathrm{Erf}\Big[\frac{\pi}{2}\sqrt{\frac{A_0}{2D}}\Big]}, \tag{S40}$$

$$p(x, x) = 0. \tag{S41}$$

This problem has the solution

$$p(x,y) = \frac{1}{2\mathrm{Erf}\Big[\frac{\pi}{2}\sqrt{\frac{A_0}{2D}}\Big]}\Big(\mathrm{Erf}\Big[y\sqrt{\frac{A_0}{2D}}\Big] - \mathrm{Erf}\Big[x\sqrt{\frac{A_0}{2D}}\Big]\Big). \tag{S42}$$

Now we are ready to understand Figure 1 in the main text. Let y be a fixed amount Δ greater than x. Equation S42 becomes

$$p(x, x+\Delta) = \frac{1}{2\int_0^{\pi/2} \exp\Big(-\frac{A_0}{2D}t^2\Big)dt}\Big(\int_x^{x+\Delta} \exp\Big(-\frac{A_0}{2D}t^2\Big)dt\Big). \tag{S43}$$

To first order in Δ, we have

$$p(x, x+\Delta) \approx \frac{\Delta \exp\Big(-\frac{A_0}{2D}x^2\Big)}{2\int_0^{\pi/2} \exp\Big(-\frac{A_0}{2D}t^2\Big)dt}. \tag{S44}$$

This is the Gaussian probability distribution observed in our simulations, with a variance of D/A_0. The denominator, upon extending the integration limits to $\pm\infty$, normalizes the numerator, and we are led to Equation 6 in the main text,

$$p(x, x+\Delta) \approx \Delta \cdot \mathcal{N}(x|x_s, D/A_0). \tag{S45}$$

where $\mathcal{N}$ is the normal distribution.

E. Turbulent Velocity Field

We generate a synthetic turbulent velocity field as in Ref. [8] using the Sabra shell model. Shells with wavenumbers $k_n = 2^{n-1}$, with $n = 1, 2, ..., 25$ each have a complex, time-dependent velocity u_n. Parameters were chosen to mimic the intermittency of the three dimensional Navier-Stokes equation (free parameter $\delta = 0.4$).

For simulations in which we do not wish to have an identical flow for each realization, a random phase is added to each shell velocity and the model is evolved for twenty times the largest shell turnover time prior to introducing organisms. This protocol ensures that the phases satisfy the equations of motion, and that we obtain a statistically independent velocity field.

A real space velocity field is obtained through a modified Fourier transform, where we construct the longest wavelength mode out of both u_1 and u_2 to create a broader palette of flow realizations,

$$u(x,t) = A_0\Big(\frac{1}{4}\big[u_1 e^{ik_1 x} + u_1^* e^{-ik_1 x}\big] + \sum_{n=2}^{25}\big[u_n e^{ik_{n-1}x} + u_n^* e^{-ik_{n-1}x}\big]\Big). \tag{S46}$$

This procedure produces a Reynolds number of approximately 2×10^6 for $A_0 = 1$.

F. The Effect of Turbulent Dynamics

In our main results (Figures 5 and 6 of the main text), for each independent simulation, we initialize organisms randomly according to a uniform distribution in the correct proportions (10% purple, 90% green). In addition to this, each simulation has an independent flow field, which we solve for by adding a random phase as described above. This gives us results that do not depend on the particular initial condition of our shell model.

However, one way that we can examine the effect of dynamics is to find the fixation probability in the presence of a single flow field time series, rather than an ensemble. In this case, the initial organism positions are still set independently at the beginning of each simulation, but the flow field at each point in time is the same between trials. We can then compare the fixation probabilities for different flows, and try to connect differences in the genetic outcomes to differences in the flows.

We show an example of this in Figure S3. As in Figure 1 of the main text, we vary the initial location of one particular species and gather fixation statistics as a function of space. The two figures shown are for two specific turbulent time series, each pictured in the inset. We see that when long-lived sources fluctuate about a mean position, successful fixation attempts are localized around these source regions much like in the case of the stationary sine wave, strongly suggesting a reduction in the effective population size. However, when these sources move quickly across the system, successful fixation attempts can originate at many locations, and the effective population size suffers a more modest reduction.

In general, the average fixation time for the systems we have studied is significantly longer than the largest eddy turnover time in our turbulence model.

G. Reynolds Number Scaling

To find the Reynolds number dependence of our effective population size, we focus on the quantity

$$n_s \tau_s \sim \langle(\partial_x v)^2\rangle^{1/2}\langle(\partial_x v)^{-2}\rangle^{1/2}. \tag{S47}$$

In the main text, neglecting intermittency effects, we argue that we can approximate this quantity as 1. Here, we calculate the effect of intermittency, and find that it introduces a non-trivial scaling with Re.

Using the multifractal approach, we assume that the statistical properties of velocity fluctuations at scales r and R ($r < R$) are given by

$$\delta v(r) = \delta v(R) \left[\frac{r}{R}\right]^h, \tag{S48}$$

with probability $P_h(r/R) \sim (r/R)^{3-D(h)}$. We use S48 to write the condition for dissipation effects to become relevant as

$$\frac{\delta v(r) r}{\nu} = \frac{\delta v(R) R}{\nu} \left[\frac{r}{R}\right]^{1+h} \sim 1. \tag{S49}$$

We label the dissipation scale $\eta(h)$. Letting $R = L$, the system size, we find

$$\eta(h) = Re^{-\frac{1}{1+h}} L, \tag{S50}$$

which is true with probability $(\eta(h)/L)^{3-D(h)} = Re^{-\frac{3-D(h)}{1+h}}$.

Now, we can use the above formulation to compute the scaling behavior in Re of moments of velocity gradients:

$$\langle (\nabla v)^p \rangle = \int dh \frac{\delta v(h)^p}{\eta(h)^p} Re^{-\frac{3-D(h)}{1+h}} \sim \left[\frac{\delta v(L)}{L}\right]^p \int dh Re^{-\frac{p(h-1)+3-D(h)}{1+h}} \sim \left[\frac{\delta v(L)}{L}\right]^p Re^{\chi(p)} \tag{S51}$$

where

$$\chi(p) = sup_h[-(p(h-1) + 3 - D(h))/(1+h)]$$

From eq. (S51) it follows that

$$n_s \tau_s \sim Re^{\alpha} \tag{S52}$$

where

$$\alpha = \frac{\chi(2) + \chi(-2)}{2}$$

We can evaluate $\chi(p)$ using our knowledge of the anomalous scaling in homogeneous and isotropic turbulence for small p. The final result reads:

$$n_s \tau_s \sim Re^{0.08} \tag{S53}$$

Eq. (S53) tells us that, beyond the mean field approach in which $n_s \tau_s = \text{const.}$, a Reynolds number dependence shows up. However, this dependence is very weak.

A detailed discussion of the multifractal formulation can be found in a recent review paper [9].

---

[1] Simone Pigolotti, Roberto Benzi, Prasad Perlekar, Mogens Høgh Jensen, Federico Toschi, and David R Nelson. Growth, competition and cooperation in spatial population genetics. *Theoretical Population Biology*, 84:72–86, 2013.

[2] Thiparat Chotibut and David R Nelson. Evolutionary dynamics with fluctuating population sizes and strong mutualism. *Physical Review E*, 92(2):022718, 2015.

[3] Simone Pigolotti, Roberto Benzi, Mogens H Jensen, and David R Nelson. Population genetics in compressible flows. *Physical Review Letters*, 108(12):128102, 2012.

[4] Hannes Risken. *The Fokker-Planck Equation*. Springer, 1996.

[5] Crispin Gardiner. *Stochastic Methods: A Handbook for the Natural and Social Sciences*. Springer Series in Synergetics, 2009.

[6] Takeo Maruyama. A simple proof that certain quantities are independent of the geographical structure of population. *Theoretical Population Biology*, 5(2):148–154, 1974.

[7] Francisco Herrerías-Azcué, Vicente Pérez-Muñuzuri, and Tobias Galla. Stirring does not make populations well mixed. *Scientific Reports*, 8(1):4068, 2018.

[8] Roberto Benzi and David R Nelson. Fisher equation with turbulence in one dimension. *Physica D: Nonlinear Phenomena*, 238(19):2003–2015, 2009.

[9] Roberto Benzi and Luca Biferale. Homogeneous and isotropic turbulence: A short survey on recent developments. *Journal of Statistical Physics*, 161(6):1351–1365, 2015.

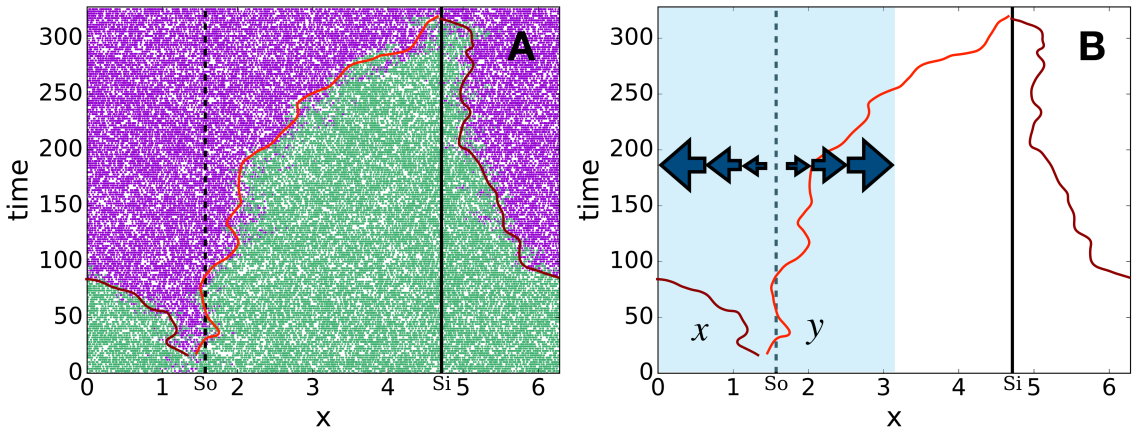

FIG. S1. Set-up for random walk approximation in a sine wave flow, with source (So) marked by the dashed line and sink (Si) marked by the solid line. (A): One realization of competition between two species in a sine wave flow, with genetic boundaries traced in light/dark red. (B): The half domain used in Figure S2, with random walkers x and y labeled. Arrows emphasize that the flow magnitude increases away from the source.

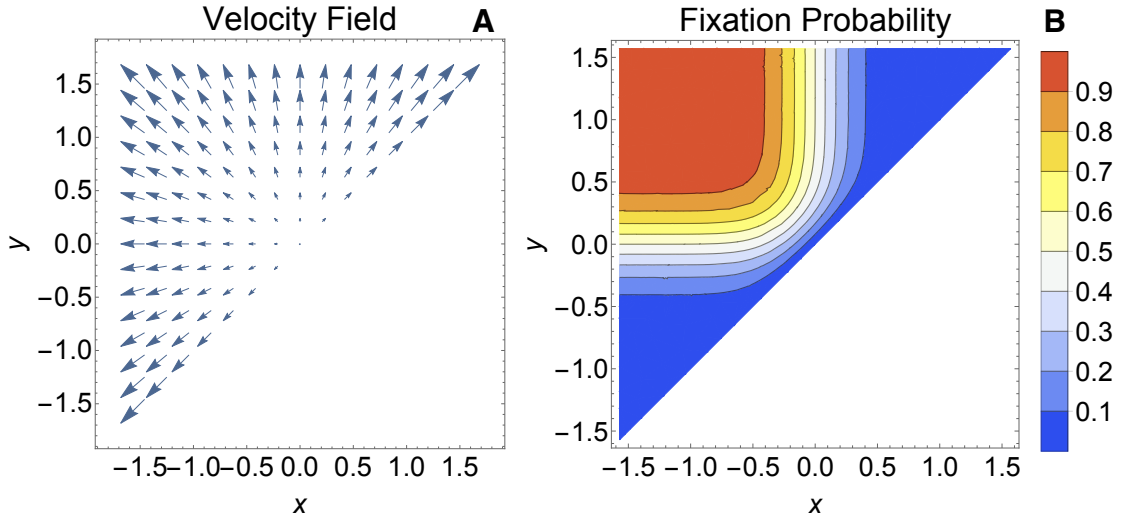

FIG. S2. (A): Spatially dependent biasing velocity field for a two dimensional random walk problem on a triangular domain. $x \in [-\pi/2, \pi/2]$ and $y \in [x, \pi/2]$. (B): Fixation probability as a function of initial position.

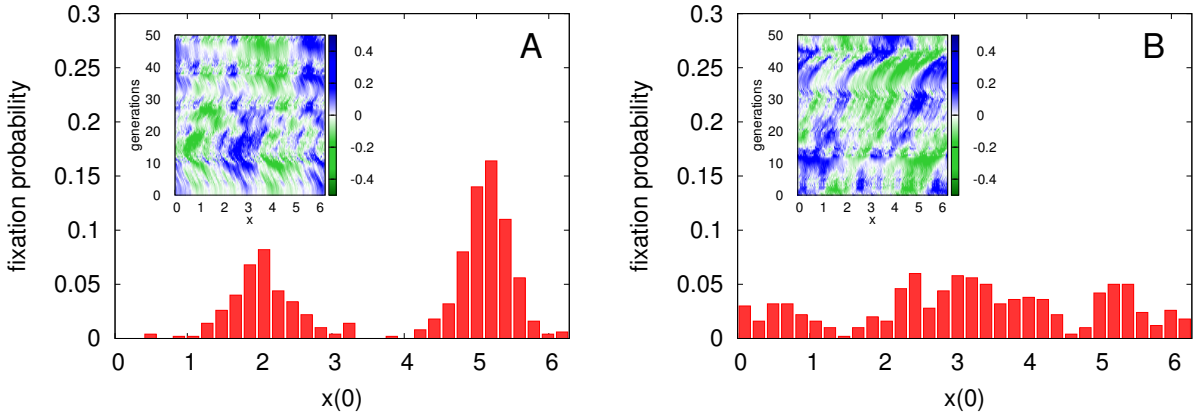

FIG. S3. Fixation probability as a function of initial position for two specific velocity time series generated using the one-dimensional shell model of compressible turbulence. Each figure shows 500 realizations for two neutral species subjected to the turbulent velocity field pictured in the inset. The color bar shows the magnitude of the velocity at each point in time and space. Sources are represented by locations where there is green on the left and blue on the right (G|B = a positive slope zero crossing). The locations that sources reach have an enhanced probability of being the origin of a successful fixation attempt. Conversely, fixation is less successful in the vicinity of sinks (= B|G) (A): In this case, significant sources fluctuate about a mean position, creating localized source regions. (B): Significant sources in this flow realization move across the system, spreading out the distribution of successful fixation attempts.